

Computational Fluid Dynamics Investigation of the Impact of Wall Treatment on Fluidization in a Liquid-Solid Fluidized Bed

C. Amuta¹, G.N. Nwaji^{1*}, N.V. Ogueke^{1,2}, E.E. Anyanwu¹

¹Mechanical Engineering Department, Federal University of Technology Owerri,
P.M.B 1526, Owerri, Nigeria

²African Centre of Excellence on Future Energies and Electrochemical systems (ACE-FUELS),
Federal University of Technology Owerri, Nigeria

ABSTRACT: This work investigates the influence of wall treatment on the prediction accuracy of the $k-\epsilon$ and $k-\omega$ models, as well as the solid volume fraction, in a solid-liquid fluidized bed. The objective of the study is to explore the effects of different y^+ values on the performance of these turbulence models and the prediction of solid-liquid fluidized bed behavior. Using the Eulerian-Eulerian approach, a multiphase flow model was employed to simulate the behavior of solid particles and liquid in a fluidized bed. The standard conservation equations of continuity and momentum were solved to describe the flow dynamics. The research findings indicate that the $k-\epsilon$ model exhibits higher sensitivity to near-wall mesh refinement when predicting y^+ values compared to the $k-\omega$ model. The $k-\omega$ model, however, demonstrates reasonably accurate predictions within the y^+ range of 30 to 45. Furthermore, the $k-\epsilon$ model outperforms the $k-\omega$ model in predicting solid volume fractions when the near-wall region is refined. These results highlight the significance of wall treatment and near-wall mesh refinement in accurately predicting turbulent flow behavior in liquid-solid fluidized beds. The study contributes to a better understanding of the performance of turbulence models and their applicability to solid liquid fluidized beds.

KEYWORDS: Near-wall, treatment, turbulence, liquid-solid, fluidized beds, volume fraction, multiphase, mesh refinement

<https://doi.org/10.29294/IJASE.10.2.2023.3388-3397> ©2023 Mahendrapublications.com, All rights reserved

1.0 INTRODUCTION

Turbulence is a common feature of any fluidized bed set-up. It causes a chaotic and irregular motion of the particles within the fluidized medium. It is characterized by the formation of eddies, swirling patterns, and random fluctuations in velocity and pressure. When turbulent flows are bounded by walls, it usually presents an additional measurement challenge when compared to those in free shear turbulence. This results in serious design limitations and implementation. Wall effect has been found to play a big role on the minimum fluidization velocity of fluidized beds. Turbulence has also been found to affect minimum fluidization velocity [1,2]. There are other inherent challenges associated with the flow dynamics such as the steepness of the mean velocity gradient around the surface and the length and time scales of the turbulence local to the near-wall [1]. The estimation of the wall adhesion forces was carried out by Wassermann [3], he compared them with

hydrodynamic forces. The findings show that fluidization characteristics at the boundary of micro-flow due to the interplay between the ratio of surface and hydrodynamic forces and wall effects affect the minimum fluidization velocity. Liu [2] studied the minimum velocity of fluidization and minimum bubbling velocity of silica sand particles in air-blown micro fluidized beds in order to appreciate the wall effect in micro fluidized beds and, the operability and usability of micro fluidized beds. The study proposed a better combination of bed diameter and particle size in the range of the static bed heights from twenty (20) to fifty (50) millimeters for the so-called micro fluidized bed reactor devised to perform reaction(s) with minimal stress from external gas mixing and diffusion of gases.

Shukla et al. [4] investigated the effects of the dimensionality of a model (3D or 2D), flow regime (laminar or turbulent), grid mesh resolutions, and drag law on the void fraction of

*Corresponding Author: godswillmee@gmail.com

Received: 05.09.2023

Accepted: 17.10.2023

Published on: 25.11.2023

Amuta et al.,

fluidized beds. 2D simulations were found to overestimate the experimental data in terms of void fraction distribution across the flow, while 3D models showed that numerically simulated profiles of the void fraction inside the bed conform more accurately to experimentally derived values. A detailed study of myriad numerical model setups proved that for the 2D simulations of fluidized beds, there is a mix of model parameters such as specularity and restitution coefficients, numerical grid resolution, and discretization scheme for convective terms that tend to produce a good correlation between numerical and experimental results. Chang et al. [5] found that 3D simulations exhibited more sensitivity to the coefficient of restitution and the specularity coefficient than 2D simulations. However, the fluidization process in the 2D models was found to develop more quickly than that in the 3D simulation.

The effect of varying Reynolds number on flow regime of liquid fluidized beds has been studied Yao et al [6]. For particle Reynolds number less than 20, the porosity is comparatively low and the particle dynamics are mostly dominated by inter-particle collisions that bring about anisotropic particle velocity variations. When particle Reynolds number is increased further to values greater than 40, the dynamics of the particles are dominated by hydrodynamic effects, which leads to decreasing and more anisotropic particle variation in velocity. A marked increase in the anisotropy happens when the Reynolds number of particles increases from 40 to 50, and this corresponds to a transition from a regime in which collision and hydrodynamic effects are equally pronounced to a hydrodynamic-dominated regime. With the use of the Eulerian-Eulerian two-fluid approach the hydrodynamics and heat transfer coefficient on various immersed bodies in a fluidized bed were studied Fathahi et al [7]. The kinetic theory of granular flow (KTGF) was adopted to analyze the solid phase. The result showed that the spherical immersed body, known to possess a better aerodynamic shape, yielded a higher heat transfer coefficient in bubbling fluidized bed with Geldart B particles classifications. The investigation of the hydrodynamic characteristics and fluidization behaviour of coarse coal particles in a three-dimensional liquid-solid fluidized bed operating in near turbulent condition has been carried out [8].

The influence of particle size and particle density on the homogeneous or heterogeneous fluidization behaviour was investigated. The findings showed that less dense and fine particles are conveniently fluidized, showing a certain range of homogeneous expansion characteristics, while in the large and heavy particles, inhomogeneity may occur throughout the bed, including water voids and velocity fluctuations.

Daryus [9] studied the effect of kinetic Prandtl number on the k- ϵ turbulence model transport equation on the behaviour of fluidized bed flow. Factors like the pressure gradient, dissipation rate, effective viscosity of the gas and the particles in the bed were investigated. The investigation observed that turbulent model with k-Prandtl of 0.9 gives rise to the most accurate results at the superficial velocity range of 0.40 m/s - 0.70 m/s, whereas k-Prandtl of 1.1 produces the most exact results at the superficial velocity range of 0.80 m/s - 0.90 m/s. It was also observed that the decrease in the k-Prandtl number leads to a decrease in the rate of dissipation; which was the same fact with effective viscosity of the gas. There was no pronounced difference in the particle's effective viscosity with the change of k-Prandtl number. The hydrodynamic behaviour in three-phase turbulent fluidized bed contactor with reverse current air flow and non-Newtonian liquid was observed and juxtaposed with that of Newtonian liquid under the same environmental conditions [10]. The aqueous medium used was carboxy methyl cellulose and the hydrodynamic variables studied were bed pressure gradient, minimum fluidization velocity, liquid holdup, bed expansion, and gas holdup. It was reported that increasing carboxy methyl cellulose concentration increased the net drop in pressure through the bed and the liquid holdup, while the gas holdup and bed expansion were found to decrease. Simulation of the heat transfer and flow rate through a turbulent gas-solid fluidized bed using the Eulerian-Eulerian granular flow model was done [11] and it accurately predicted the chamber pressure difference, temperature change, and bed expansion.

A comparative study of the flow behaviour in three-dimensional supercritical water fluidized beds, cold gas-solid fluidized beds, and high-temperature gas-solid fluidized beds was carried out [12] employing the two-fluid model simulations across different fluid velocities. The

work also studied particle dynamics, fluid velocities, and bed expansions. The outcome showed that, the drag forces of particulate phase are about 0.4 times particulate phase weights in supercritical water fluidized beds. In contrast with supercritical water fluidized beds, cold gas-solid fluidized beds have lower minimum fluidization velocities, the size of bubble and slug were smaller, more bubble and slug numbers, higher bed expansions and slug onset heights, and more uniform gas-solid interactions. There have works on a three-dimensional simulation to obtain the voidage distributions through a time averaged simulation. The impact of superficial inlet velocity, temperature, pressure, and particle size on the radial and axial voidage, probability density of voidage, and bed expansion were investigated [13].

Abdulrahman et al., [14] adopted the Eulerian-Eulerian granular multiphase flow technique to study the performance of liquid-solid fluidized beds. The study quantified the characteristics of both the solid and liquid holdups. The findings reveal that smaller glass beads that represented the solid particles require low minimum fluidization velocity; also, this velocity requirement increased as the diameter of the bead increased. It was also found that the bed expansion ratio is directly proportional to the velocity of the liquid, and inversely proportional to the diameter of the beads. Whereas the solid holdup decreased with velocity, the liquid holdup increased with increasing liquid velocity.

Resolving near-wall regions properly is very important in capturing the effects of the different sub layers close to the wall. Wall treatment refers to the modeling approach used to simulate the behaviour of fluid flow near solid boundaries, such as walls, in numerical simulations. Accurately representing the flow near walls is essential because it influences various phenomena, including boundary layer development, wall shear stress, and heat transfer. In this work wall resolution is done by discretization of the computational domain with mesh of different sizes and is used alongside two different turbulent models, the $k-\varepsilon$ and $k-\omega$ models to study the effect of wall treatment and turbulence models on the wall y^+ values and volume fractions of the bed.

2.0 METHODOLOGY AND MATERIALS

The fluidized bed considered in this work is found in [15], as shown in Fig. 1. The continuity, momentum and energy equations governing the flow in the liquid-solid fluidized bed are solved in a 2D bed geometry using ANSYS FLUENT.

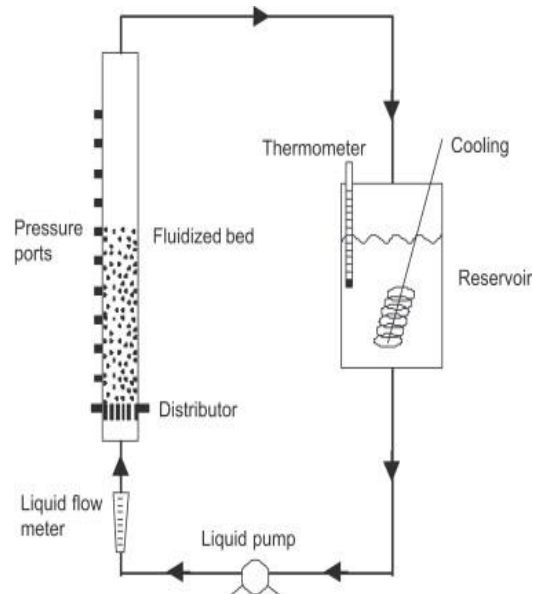


Fig. 1 Physical set-up of the modeled liquid-solid fluidized bed [15]

From Fig. 1, fluidization occurs in the bed of packed particles in a liquid medium. The bed section is idealized as a simple 2D geometry. It has a column of 0.127m diameter and height of 1.1m. The liquid is water and the particles are glass beads of 1.13mm Sauter mean diameter. The model equations were formulated based on the following assumptions (i) it is idealized as a 2D flow (ii) external body forces such as magnetic and electrostatic forces are negligible, and (iii) the solid particles are of uniform size.

Using the Eulerian-Eulerian method incorporating the kinetic theory of granular flow, the governing equations were formulated and shown in Table 1. The closure equations for the drag force are presented in Table 2. Two types of turbulence models have been studied, namely, the standard $k-\varepsilon$ and $k-\omega$ two-equation models for the resolution of the transport of kinetic energy and its dissipation rate. The standard $k-\varepsilon$ model assumes that the turbulent viscosity is isotropic, that is, the ratio of Reynolds stress and mean rate of deformation is equal in all directions. For the $k-\omega$ model, the first equation takes care of the turbulent kinetic energy while the second

accounts for the specific rate of turbulent energy dissipation. The model constants for the two turbulent models are presented in Table 3, and the fluid properties are shown in Table 4. The following boundary conditions were applied (i) inlet fluid velocity = 0.076m/s (ii) Wall roughness constant is = 0.5 (iii) backflow turbulent intensity

0.001m²/s² (iv) turbulent intensity = 5% (v) initial volume fraction = 0

The equations are solved by the student version of the commercial code ANSYS FLUENT

2022R. The model equations were solved using the turbulent flow option in 2D space and applying the second order implicit iterative method. An Intel64 bit Operating system having Pentium 8 central processing unit running on 4GHZ with 4GB RAM was used to carry out the simulation. The scalable wall treatment was applied while maintaining an absolute frame of reference. The iteration was run for two different time steps; 10000 and 20000 at a maximum of 20 iterations per time step using a time step size of 0.001secs.

Table 1: Governing equations

The continuity equations	$\frac{\partial}{\partial t}(\varepsilon_l \rho_l) + \nabla \cdot (\varepsilon_l \rho_l \mathbf{v}_l) = 0$ for the liquid phase
	$\frac{\partial}{\partial t}(\varepsilon_s \rho_s) + \nabla \cdot (\varepsilon_s \rho_s \mathbf{v}_s) = 0$ for the solid phase
The momentum equations	$\frac{\partial}{\partial t}(\varepsilon_l \rho_l \mathbf{u}_l) + \nabla \cdot (\varepsilon_l \rho_l \mathbf{u}_l) = -\varepsilon_l \nabla P + \nabla \cdot \boldsymbol{\tau}_l + \varepsilon_l \rho_l \mathbf{g} + \beta(\mathbf{u}_l - \mathbf{u}_s)$ for the liquid phase
	$\frac{\partial}{\partial t}(\varepsilon_s \rho_s \mathbf{u}_s) + \nabla \cdot (\varepsilon_s \rho_s \mathbf{u}_s) = -\varepsilon_s \nabla P + \nabla \cdot \boldsymbol{\tau}_s + \varepsilon_s \rho_s \mathbf{g} + \beta(\mathbf{u}_s - \mathbf{u}_l)$ for the solid phase

Table 2: Closure equations

Liquid solid drag	$C_d = 150 \frac{\varepsilon_s(1 - \varepsilon_l)\mu_l}{\varepsilon_l d_s^2} + 1.75 \frac{\varepsilon_s \rho_l v_s - v_l }{d_s}$	Gidaspow et al, 1992 [16]
solid pressure	$P_s = \alpha_s \rho_s \theta_s + 2\rho_s(1 + e_{ss})\alpha_s^2 g_{o,ss} \theta_s$	Symal et al, 1993 [17]
Radial distribution	$g_o = [1 - (\frac{\alpha_s}{\alpha_{smax}})^{\frac{1}{3}}]^{-1}$	Ogawa et al, 1980[18]
solid shear stress	$\mu_s = \mu_{s,col} + \mu_{s,kin} + \mu_{s,fr}$ $\mu_{s,col} = \frac{4}{5} \alpha_s \rho_s d_s g_{o,ss} (\frac{\theta_s}{\pi})^{1/2} \alpha_s$ $\mu_{s,kin} = \frac{\alpha_s d_s \rho_s \sqrt{\theta_s} \pi}{6(3 - e_{ss})} [1 + \frac{2}{5}(1 + e_{ss})(3e_{ss} - 1)\alpha_s g_{o,ss}]$ $\mu_{s,fr} = \frac{P_s \sin \phi}{2\sqrt{I_2} D}$	Gidaspow et al, 1992 [16] Symal1993 [17] Schaeffer, 1987 [19]
Bulk viscosity	$\lambda_s = \frac{4}{3} \alpha_s \rho_s g_{o,ss} (1 + e_{ss}) (\frac{\theta_s}{\pi})^{\frac{1}{2}}$	Lun et al, 1984 [20]

Granular temperature	$\frac{3}{2} \left[\frac{\partial}{\partial t} (\rho_s \alpha_s \theta_s) + \nabla \cdot \rho_s \alpha_s \theta_s v_s \right] = (-P_s I + \tau_s) : \nabla v_s + \nabla \cdot (k \theta_s \nabla v_s) - \gamma \theta_s + \psi \theta_s$	Symal et al 1993[17]
----------------------	---	----------------------

Table 3: Closure constants for the $k - \varepsilon$ and $k - \omega$ models

$k - \varepsilon$	$k - \omega$
$\sigma_k = 1.0$	
$\sigma_\varepsilon = 1.30$	$\alpha = 0.56$
$C_{1\varepsilon} = 1.44$	$\beta = 0.3$
$C_{2\varepsilon} = 1.92$	$\beta^* = 0.9$

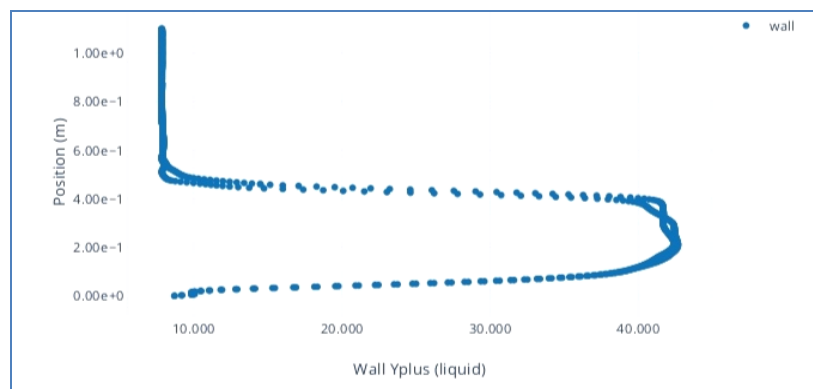
Table 4: Fluid and solid Properties

Liquid phase	
Density	999.5Kg/m ³
Specific heat capacity	1006J/kg.K
Viscosity	0.001236Kg/m.s
Molecular weight	28.966Kg/Kmol
Thermal conductivity	0.0242W/m.K
Solid phase	
Density	2540Kg/m ³
Sauter diameter	1.13e-3 m
Packed bed volume fraction	0.6

3. RESULTS AND DISCUSSION

The results obtained from the study are presented and discussed in Figs. 2-8. The y^+ values represent the distance from a computational grid point to the nearest wall,

normalized by a characteristic length scale in the flow. It provides information about the flow physics near the wall and is used to determine the appropriate grid resolution in the near-wall region.

Fig. 2 Variation of y^+ values with bed height for $k - \varepsilon$ turbulence model at 2.5mm grid size

Amuta et al.,

Fig. 2 shows the variation of y^+ values against bed height for 2.5mm grid size. It can be seen that the values increase with bed height and reached well over 40 within a short distance of the bed height, and thereafter started decreasing until it reached 10 at about 0.5m bed height. Above 0.5m, the y^+ values maintained a constant value. This means that the first

computational cell centroid is located relatively far away from the wall. The y^+ value of 40 falls within the "log-law" region, which is relatively far from the wall and outside the viscous sublayer. This suggests that a global mesh size of 2.5mm has a coarse resolution near the wall which might compromise near-wall prediction.

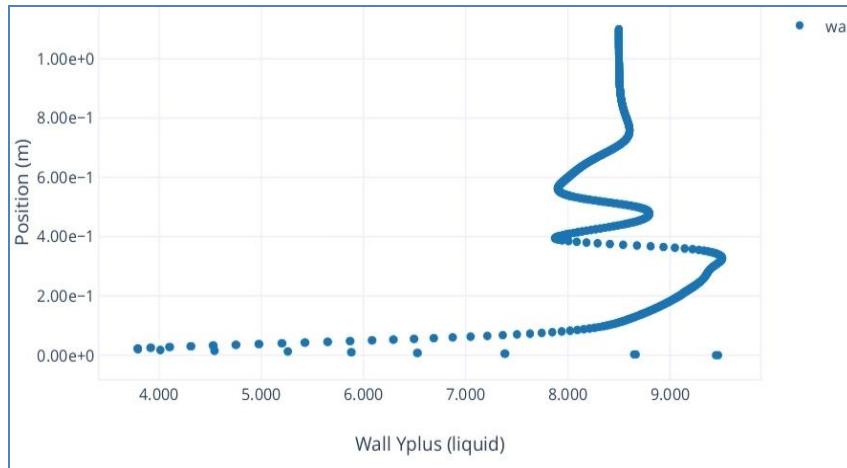


Fig. 3 Variation of y^+ values with bed height for $k-\epsilon$ turbulence model for 2.5mm grid size with a refined mesh at the wall

Fig. 3 shows the effect of near-wall mesh refinement on the turbulence. From the wall, the y^+ values increased with bed height until at about 0.3m when it became unstable with almost unnoticeable marginal increase. The maximum y^+ value was as low as 9.3, indicating that near-wall flow behaviour, and resolution of the effect of viscosity and velocity gradient can be done with high fidelity.

For the $k-\epsilon$ model with a mesh size of 1.25mm shown in Fig. 4, there is no marked uniformity in the pattern of variation of the y^+ values near the wall. However, a maximum value of about 25 can be observed. This suggests that the first computational cell centroid is located within the viscous sublayer, and it shows a clear difference of over 50% compared to the 2.5mm mesh.

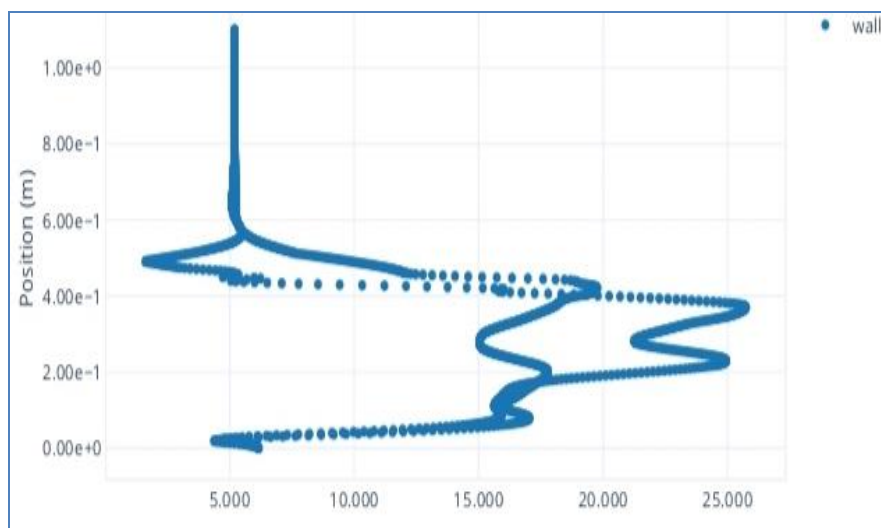


Fig. 4: Variation of y^+ values with bed height for $k-\epsilon$ turbulence model at 1.25mm grid size

The $k-\omega$ model gave a lower y^+ value of about 35 as can be seen in Fig. 5 for the 2.5mm mesh size which suggests better resolution of near-wall region. When the global mesh size was changed to 1.25mm, the y^+ values for the $k-\omega$ model moved closer to the 30 mark as shown in Fig. 6. It is evident that the $k-\varepsilon$ model showed

more sensitivity to near wall mesh refinement than the $k-\omega$ model in predicting the y^+ values. Past authors have suggested different wall y^+ resolutions for near-wall flows. Reports of available work have been compiled and compared with the present work as shown in Table 5.

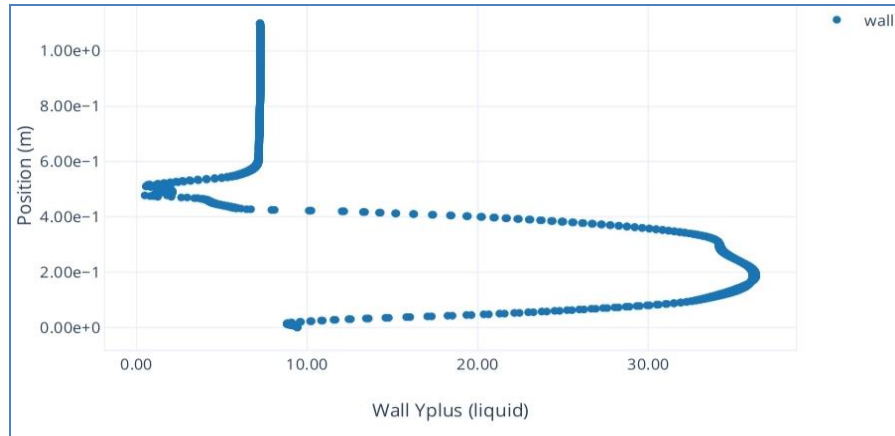


Fig. 5: Variation of y^+ values with bed height for $k-\omega$ turbulence model at 2.5mm grid size

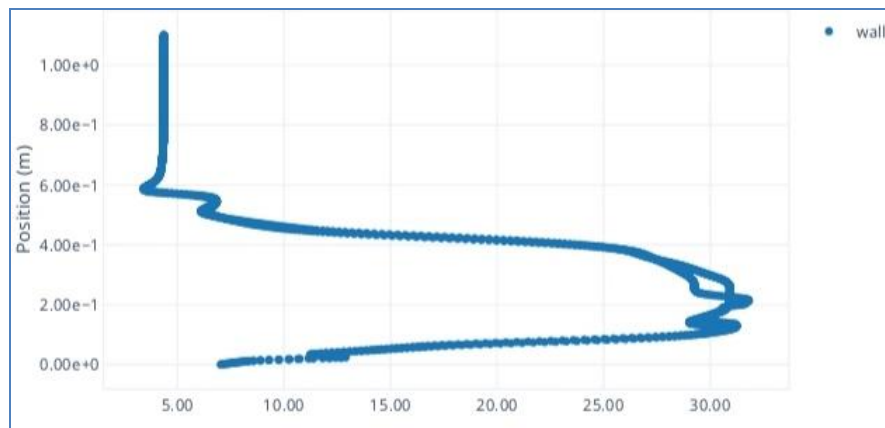


Fig. 6: Variation of y^+ values with bed height for $k-\omega$ turbulence model at 1.25 grid mesh

Table 5: Comparison of different near wall treatments and y^+ values with present work

Authors	Year	Turbulence	Near wall treatment (s)	Y^+ values
Muhammad [21]	2019	$k-\varepsilon$	Standard wall function	8.7
Salim et al [22]	2009	$k-\varepsilon$	Standard wall function	$30 < y^+ < 60$
Saverio et al [23]	2018	not specified	Not specified	$30 < y^+ < 100$
Present work	2023	$k-\varepsilon$	Standard wall function	$9.3 < y^+ < 45$
		$k-\omega$	Standard wall function	$30 < y^+ < 40$

The vector plot of volume fractions in the bed is shown in Figs 7 and 8. It shows that the

magnitude of fluctuations of liquid volume fraction is higher for both the $k-\varepsilon$ and $k-\omega$

Amuta et al.,

models near the wall. This is consistent with the findings of Marefatallah et al [24] which showed that the highest magnitude of fluctuation is

usually around the near-wall region and can be up to 3 to 4 times greater than that at the center of the bed.

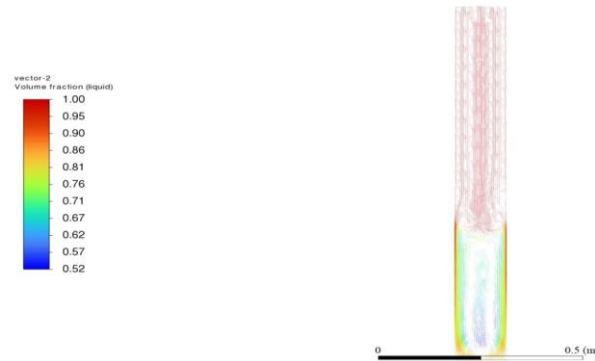


Fig. 7: Vector plot of volume fraction for $k-\epsilon$ model and 2.5mm mesh

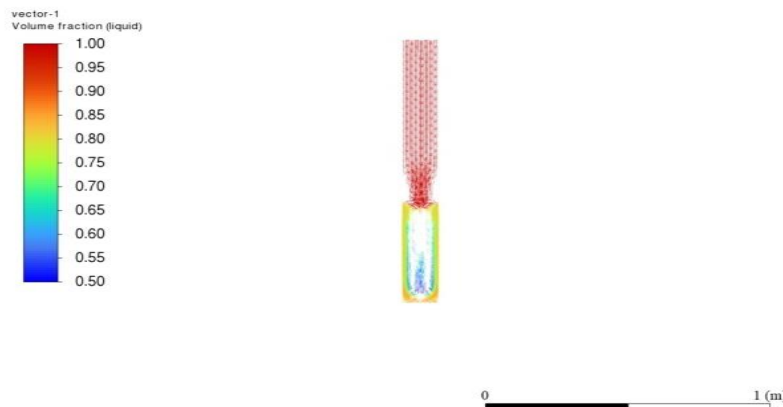


Fig. 8: Vector plot of volume fraction for $k-\omega$ model and 2.5mm mesh

4.0 CONCLUSION

A numerical simulation of the near-wall treatment in a liquid-solid fluidized bed has been undertaken. From the two comparative simulations carried out involving $k-\epsilon$ and $k-\omega$ models, it was observed that the $k-\epsilon$ model showed more sensitivity to near wall mesh refinement than the $k-\omega$ model in predicting the y^+ values. The $k-\omega$ model gives a reasonably accurate prediction in the range of $30 < y^+ < 45$. The best prediction of liquid volume fraction was made by the $k-\epsilon$ model when the near-wall region was refined. This means that different turbulence models have different capabilities and promises in the prediction of the accuracy of numerical simulations of multiphase flows, and the choice of a more appropriate model solely depends on the particular parameter of interest. This study, therefore, establishes the fact the $k-\epsilon$ and $k-\omega$ models are good closure models for two-

phase flows in liquid-solid fluidized beds. However, it is suggested that more turbulence models be studied and perhaps further refinements near the wall be done to establish the best model for the fidelity of CFD simulations of fluidization process in fluidized beds.

Definition of symbols

Symbol	Meaning
τ	Phase stress-strain tensor,
β	Interphase momentum exchange coefficient
$g_{o,ss}$	Radial distribution function
e_{ss}	Coefficient of restitution for particle collisions
θ_s	Granular temperature
V_T	Kinematic viscosity
ϵ	Volume fraction
ρ	Density
v	Velocity
g	Gravitational acceleration
μ	Shear viscosity

Amuta et al.,

P	Pressure
γ	Bulk viscosity
η	Dynamic viscosity
Re	Reynolds number

Acknowledgments

The authors wish to sincerely appreciate the Applied Energy Research Group and Department of Mechanical Engineering, Federal University of Technology Owerri for the assistance in acquiring the resources used for this work.

REFERENCES

- [1] Klewicki, J., Saric, W., Marusic, I., Eaton, J., 2007. Wall-Bounded Flows. In: Tropea, C., Yarin, A.L., Foss, J.F. (eds), Springer Handbook of Experimental Fluid Mechanics. Springer Handbooks. Springer, Berlin, Heidelberg.
- [2] Liu G, 2018. Application of the Two-Fluid Model with Kinetic Theory of Granular Flow in Liquid-Solid Fluidized Beds. Granularity in Materials Science. In Tech. Available at: <http://dx.doi.org/10.5772/intechopen.79696>.
- [3] Wasserman, S., 2016 Choosing the Right Turbulence Model for Your CFD Simulation. Engineering.com retrieved from <https://www.engineering.com/story/choosing-the-right-turbulence-model-for-your-cfd-simulation>. Accessed on 5th January, 2023
- [4] Shukla, I., Tupkari, S., Raman, A., Mullick, A., 2012. Wall Y plus Approach for dealing with Turbulent Flow through a Constant Area Duct. Powder Technology, Pp. 144-153. 10.1063/1.4704213. Accessed on 17th March, 2023
- [5] Chang, O. Talib, D. Michel, W. Damien, M., Marc L., 2019. Liquid-solid two-phase jet in a turbulent cross flow: Experiments and simulations. 03224997, Chemical Engineering Science, 56(2) 571-578
- [6] Yinuo, Y., Craig, S., Oliver, B. 2021. Competing flow and collision effects in a monodispersed liquid-solid fluidized bed at a moderate Archimedes number, Journal of Fluid Mechanics , 25 November, A28
- [7] Fattahi, M., Seyyed, H., Goodarz, A., Arsalan, P., 2019. Numerical simulation of heat transfer coefficient around different immersed bodies in a fluidized bed containing Geldart B particles, International Journal of Heat and Mass Transfer, 141, 353-366.
- [8] Peng, J., Sun, W., Han, H., Xie, L., 2021. CFD Modeling and Simulation of the Hydrodynamics Characteristics of Coarse Coal Particles in a 3D Liquid-Solid Fluidized Bed. Minerals, 11, 569.
- [9] Daryus, A., Siswantara, A., Budiarto, Sumartono, B., Gunadi, G.G., Pujowidodo, H., Widiawaty, C., 2019. CFD simulations of complex fluid flow in gas-solid fluidized bed using modified k- ϵ turbulence models. The 4th biomedical engineering's recent progress in biomaterials, drugs development, health, and medical devices: Proceedings of the International Symposium of Biomedical Engineering (ISBE)
- [10] Syed, S., Ila, A., Zaman, M., Chughtai, I., Inayat, M., 2017. Counter-current three-phase fluidization in a turbulent contact absorber: A CFD simulation Particology. 35, 51-67
- [11] Potgieter, A., Bhamjee, M., Kruger, S., 2021. Modelling of a Heated Gas-solid Fluidised Bed using Eulerian Based Models. R&D Journal, 37, 45-57
- [12] Xie, L. Zheng-Hong L., 2018. Modeling and simulation of the influences of particle-particle interactions on dense solid-liquid suspensions in stirred vessels, Chemical Engineering Science, 176, 439-453,
- [13] Wu Z, Jin H, Ou G, Guo L, Cao C. Three-dimensional numerical study on flow dynamics characteristics in supercritical water fluidized bed with consideration of real particle size distribution by computational particle fluid dynamics method. Advances in Mechanical Engineering. 2018;10(6).
- [14] Abdulrahman, A.A., Mahdy, O.S., Sabri, L.S., Sultan, A.J., Al-Naseri, H., Hasan, Z.W., Majdi, H.S., Ali, J.M., 2022. Experimental Investigation and Computational Fluid Dynamic Simulation of Hydrodynamics of Liquid-Solid Fluidized Beds. Chem Engineering 6, 37. Pp. 1-18.
- [15] Cornelissen, J., Fariborz, T., Renaud, E., Naoko, E., John R., 2007. CFD modelling of a liquid-solid fluidized bed, Journal of Chemical Engineering Science 62, 6334 – 6348
- [16] Gidaspow, D., Bezburuah, R., Ding, J., 1992 Hydrodynamics of Circulating Fluidized

- Beds, Kinetic Theory Approach In Fluidization VII, Proceedings of the 7th Engineering Foundation Conference on Fluidization, pages 75-82.
- [17] Syamlal, R.W., O'Brien T., 1993. MFIx Documentation: Volume 1, Theory Guide. National Technical Information Service, Springfield, VA, DOE/METC-9411004, NTIS/DE9400087.S.
- [18] Ogawa, A., Oshima, N., 1980. On the Equation of Fully Fluidized Granular Materials. J. Appl. Math. Phys., 31:483
- [19] Schaeffer, G., 1987. Instability in the Evolution Equations Describing Incompressible Granular Flow. J. Diff. Eq., 66:19-50. Retrieved from: <https://www.afs.enea.it/project/neptunius/docs/fluent/html/th/node420.html>.
- [20] Lun, C., Savage, B., Jeffrey, D., Chepur, N., 1984. Kinetic Theories for Granular Flow: Inelastic Particles in Couette Flow and Slightly Inelastic Particles in a General Flow Field. J. Fluid Mech., 140, 223-256.
- [21] Mohamed, S., 2016. Experimental study on the effect of active engine thermal management on a bi-fuel engine performance, combustion and exhaust emissions, Applied Thermal Engineering, 106,1352-1365.
- [22] Salim, M., Cheah, S., 2009. Wall y+ Strategy for Dealing with Wall-bounded Turbulent Flows. Lecture Notes in Engineering and Computer Science. 2175.
- [23] Saverio, F., Giordana, G., 2018. Indicators for the Quality Assessment of the Grid Resolution. IOP Conf. Series: Journal of Physics: Conf. Series 1107,042025
- [24] Marefatallah, M., David, B.R., Sean S., 2021. Experimental study of local solid volume fraction fluctuations in a liquid fluidized bed: Particles with a wide range of stokes numbers, International Journal of Multiphase Flow, 135, 103348.